

Parallel Computing Application on Combustion and Emission Analysis of an Annular Gas Turbine Combustor

Hong-Gye Sung¹, Won-Cheol Jeong¹ and Sung Yoon Kim²

¹High Speed Propulsion and Combustion Control Laboratory Korea Aerospace University
Goyang, Gyeonggi, 412-791, South Korea
hgsung@kau.ac.kr

Abstract

To analyze the emissions of a turbulent lean premixed Methane-air combustor, a level set G-equation method has been implemented in the Large Eddy Simulation (LES) framework using parallel personal server. The server consists of 36 nodes with 12 CPU cores a node. GRI-MECH 3.0 which is a compilation of 325 elementary chemical reactions with 53 species, has been used with Presumed-Probability Density Function (PDF) method. The combustion flames from each injector move extremely dynamically and rotate in different directions from adjacent injectors because the swirl directions of each injector are opposite to the adjacent injectors. CO has high concentration on the flame and disappears rapidly after the flame due to the lean premixed conditions. NO mole fraction increases continuously after the flame and then is emitted at the exit of combustor.

1. Introduction

The combustion process generally emits several pollutants, such as nitrogen oxide, carbon oxide, and so on, which have detrimental effects on both human health and our environment. Over the years, carbon emission of fossil fuels has increased and induced global warming and raised the temperature of land-ocean. These affect environmental problems such as reducing the thickness of glaciers. With these serious problems, gas turbine engines have been especially regulated by stringent emission limits.

As part of an effort to reduce the amount of emissions as well as improve performance, lean premixed combustion has been applied to gas turbine engines. Lean-premixed combustion which premixes fuel and excess air upstream of the reaction region in order to avoid locally stoichiometric combustion is widely used to comply with the strict regulation of pollutant emission.

For these reasons, many studies of emissions predictions in lean premixed gas turbine combustor

have been conducted. Benim and Syed investigated the laminar flamelet modeling for pollutant prediction of industrial gas turbine and showed relatively good agreement with experimental data[1]. Park et al. investigated a chemical reactor network for emission prediction of a lean premixed gas turbine combustor using Computational Fluid Dynamics – Chemical Reactor Networks (CFD-CRN)[2].

Most of the previous studies on the emission prediction of gas turbine combustors have focused on the emissions of single element burners and injectors. Though the interactions between injectors and associated wall coupling are important, they have often been ignored. The purpose of the present research is to investigate the combustion dynamics and emission analysis in an annular combustor with multiple swirl injectors, which was performed an in-house personal server.

2. Parallel PC Server

2.1. Hardware

Each communication switch clusters 36 nodes with 12 CPU cores of 2.6 GHz and 64 GB RAM a node. The shared Network File System (NFS) are accessible to all nodes connected by a lower latency infiniband network. The Intel® Xeon® processor E5-2600 V2 product family, codenamed “Ivy Bridge EP”, is a 2-socket platform based on Intel’s most recent microarchitecture

2.2. Software

For job scheduling to allocate computational tasks, i.e., batch jobs, among the available computing resources, Portable Batch System (PBS) is applied. There are three compiler flavors available on the cluster: 1) the standard GNU compilers supplied with Linux, 2) the Intel compilers, and 3) the Portland Group compilers. GNU, Intel and Portland Group Compilers are available for High Performance Fortran

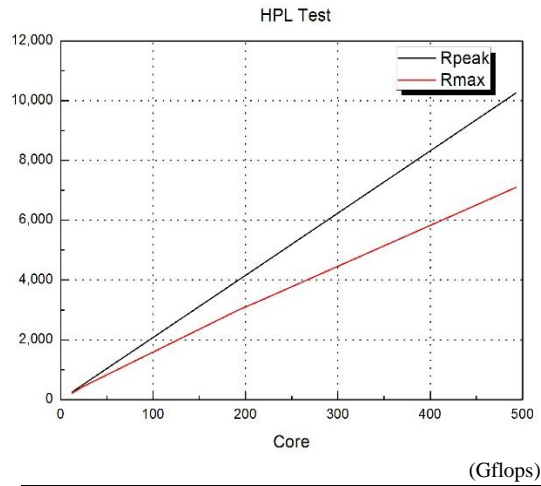
(HPF), C, C++ and OpenMP compilers, debuggers and profilers.

The Cluster offers a choice of message passing libraries, including Message Passing Interface (MPI) libraries (Open MPI, MPICH, Intel-MPI) optimized for high-speed interconnects such as InfiniBand.

2.3. Benchmark

The LINPACK Benchmarks are a measure of a system's floating point computing power. The maximum theoretical GFLOPS (billion floating point operations per second) per system is depending on the number of cores, clock speed and IPC's (instructions per cycle).

For 36 node tests we have compared the performance obtained with server's default Advanced Vector Extension (AVX) configurations.



Core	12	24	192	216	493
Rpeak	249	499	3,993	4,492	10,254
Rmax	219	431	3,000	3,307	7,100

Figure 1. HPL Test Result

- Rpeak: the theoretical peak performance Gflop/s for the machineN.
- Rmax: the performance in Gflop/s for the largest problem run on a machine

Even though the result of the test is slightly lower than theoretical performance, it is may unable to grow large problem size to the performance.

3. Combustion and Emission Application

3.1. Theoretical and Numerical Formulation

The governing equations based on the Favre filtered conservation equations of mass, momentum, and energy in three dimensions can be written as:

$$\frac{\partial \bar{\rho}}{\partial t} + \frac{\partial \bar{\rho} \tilde{u}_j}{\partial x_j} = 0 \quad (1)$$

$$\frac{\partial \bar{\rho} \tilde{u}_i}{\partial t} + \frac{\partial (\bar{\rho} \tilde{u}_i \tilde{u}_j + \bar{p} \delta_{ij})}{\partial x_j} = \frac{\partial (\bar{\tau}_{ij} - \tau_{ij}^{sgs})}{\partial x_j} \quad (2)$$

$$\frac{\partial \bar{\rho} \tilde{E}}{\partial t} + \frac{\partial ((\bar{\rho} \tilde{E} + \bar{p}) \tilde{u}_i)}{\partial x_i} = \frac{\partial}{\partial x_i} (\tilde{u}_j \bar{\tau}_{ij} + \bar{q}_i - H_i^{sgs} + \sigma_{ij}^{sgs}) \quad (3)$$

where i and j are the spatial coordinate index and are the viscous stress tensor and heat flux, respectively. SGS is the unresolved sub-grid scale (sgs) closure term.

The Favre filtered G equation is modeled by a level-set equation:

$$\frac{\partial \bar{\rho} \tilde{G}}{\partial t} + \nabla \cdot \bar{\rho} \tilde{\mathbf{u}} \tilde{G} = -\bar{\rho} D_i \tilde{k} |\nabla \tilde{G}| + \bar{\rho} S_T |\nabla \tilde{G}| \quad (4)$$

The sgs turbulent flame velocity, S_T , is modeled as:

$$S_T = S_L \left(C \left[\left(\frac{P}{P_0} \right) \left(\frac{u'_\Delta}{S_L} \right) \right]^n \right) \quad (5)$$

where u'_Δ is the sgs turbulent velocity fluctuation, which is assumed to be $u'_\Delta = 2.0 \Delta^3 (\nabla \times (\nabla^2 \tilde{\mathbf{u}}))$ [3]. The constants C and n can be specified as 5.04 and 0.38 respectively [4].

With the assumption that the mean turbulent flame is an ensemble average or local volume average of different laminar flamelets that fluctuate randomly around the mean flame position in the normal direction under the effect of turbulence, the mean chemical composition of a premixed turbulent flame can be obtained using a presumed Probability Density Function (PDF) method along with a resolved flamelet structure. To this end, the probability of finding the instantaneous flame front at a given position and instantly needs to be presumed. A reasonable choice appears to be a Gaussian distribution.

In the present study, a flamelet library is established by solving a system of transport equations for the temperature and species concentration fields for a freely propagation plane flame [5].

3.2. Numerical Schemes

The governing equations are numerically solved by means of a finite-volume approach. A second order central differencing scheme in generalized coordinates is used for spatial discretization. Temporal discretization is obtained using a two-step Runge-Kutta

integration scheme. A multi-block technique is used to facilitate the implementation of parallel computation with message passing interfaces at the domain boundaries [6].

3.3. Computational Condition

The present study employs the LM6000 lean premixed swirl-stabilized annular combustor; experimental data of single injector combustor are available. The LM6000 device involves co-axial multi-swirl (swirl/counter swirl) injectors

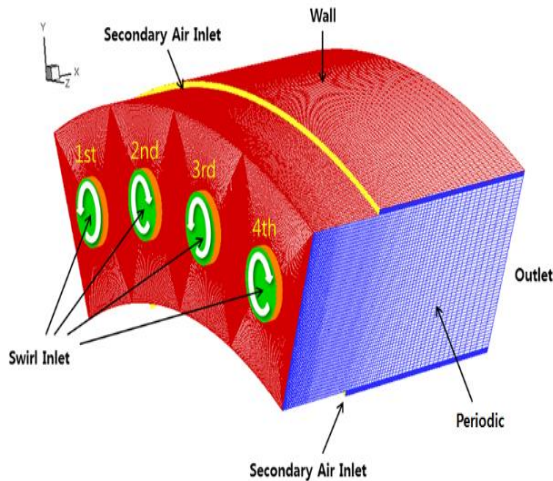


Figure 2. Schematic of Grid System and Boundary Conditions

Figure 2 shows a schematic of the computational domain, including four swirl injectors and two secondary air inlet slots. In this study, two secondary air inlet slots are not considered. Each injector measures 34mm diameter and projects 5mm from the front wall. The modified annular-type combustor is based on the single rectangular combustor[7]. Each swirl sector of the annular combustor has almost the same tangential width as the single rectangular combustor. The angle between the injectors is 12 degrees. The computational domain consists of approximately 9.2×10^6 grid points, and is divided into 136 blocks; each block is assigned to a processor.

The operating conditions are: pressure 6 atm., temperature 640 K, and overall equivalence ratio of methane-air 0.56. The specific inlet velocity profile is based on experimental data and the swirl number is about 0.56. The specific inlet velocity profile is based on experimental data from a practical swirl/counter-swirl combustor configuration. The swirl direction of each injector is counter to the direction of its neighboring injectors.

3.4. Discussion

(a) Reacting Flow Characteristics

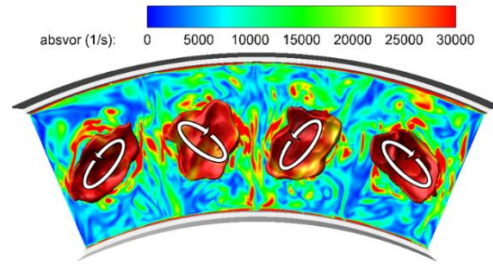


Figure 3. Instantaneous iso-flame Surface and Vorticity on y-z plane [1/s]

Flame shapes and vorticity structure of a multi injector annular gas turbine combustor are presented in figure 3. Premixed fuel is injected with different swirl direction according to adjacent injectors then mutual interaction occurs between flow from neighboring injectors. With this mutual interaction, the flame shape rotates in the opposite direction alternately between lateral injectors. The flame movement is greatly dynamical and rotates and then flame changes are observed in periodical.

Figure 3 illustrates the vorticity intensity on cross section of the combustor, which representing vorticity from each injector encountered and collapsed. Also from figure 6, which checks vorticity intensity from the top of single and multiple injector combustors, generated vorticity of single injector diffuses from the center of the injector to radial direction along the radial flame shape and spreads to the combustor axial direction. Vorticity recirculation which is detected from the corner region of single injector combustor is recycled straight and stable. On the other hand, the vorticity recirculation of multiple injectors recycled at the corner of combustor and interval space between adjacent injectors is extremely unstable and complicated. The vorticity generated from multiple injectors spreads to tangential direction of combustor, then diffused vorticity encounters and collapses so that vorticity intensity is gradually attenuated through the combustor.

(b) Emissions

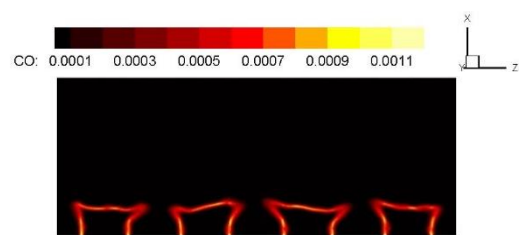


Figure 4. Time-averaged CO Concentration on x-z plane

Time-averaged CO formation shape from single and multiple injectors in the annular gas turbine combustor is shown in figure 4. Multiple injector CO formation mutually appears on the flame then disappears quickly and concentration of CO is not indicated after the flame. CO concentration is high on the flame which is attached to the injector and center of expanded flame surface because this region of flame is concentrated strongly due to corner and center vorticity recirculation so that CO is generated intensively on that region of flame. In contrast, the CO formation of multiple injectors on the flame region where it is attached to the injector is inhomogeneous because the corner and interval space of lateral injectors vorticity recirculation is unstable which makes concentration of flame relatively irregular. Owing to interaction among the injectors, a flame formation differs from others and as a result, CO concentration shapes are different from each other.

One of the pollutant, time-averaged NO distribution contours can be seen in figure 5. In the front region of the combustor, NO distributes along the shape of flame structure with respect to both single injector and multiple injector, but from the center region of multiple injector combustor's axial direction, NO distribution is hardly affected by injector interactions so spreads homogeneously in tangential direction of combustor. The proportion concentration of NO increases gradually.

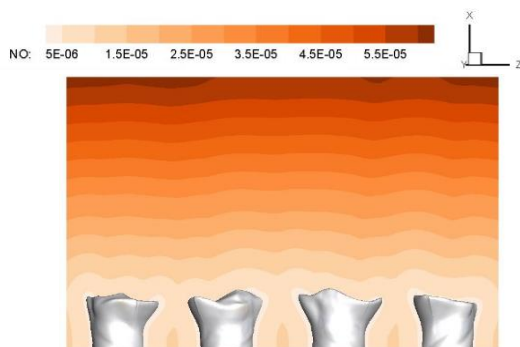


Figure 5. Time-averaged NO Concentration on x-z plane

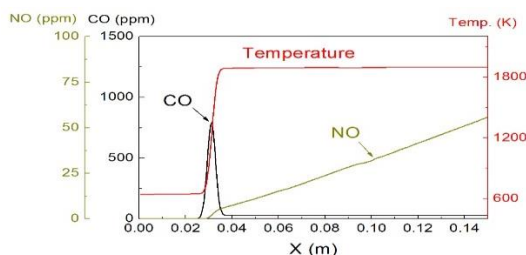


Figure 6. CO, NO and Temperature Properties Diagram from 2nd Left Injector of multiple injector combustor

For the quantitative analysis, CO, NO formation behavior is extracted from the second left injector's axial direction of the annular combustor and exhibited on the following diagrams.

Figure 6 shows that CO concentration peaks the value of 796.53ppm at the flame position of 3cm back from the injector with increasing temperature. Then CO concentration decreases sharply but the temperature keeps its value of about 1900K in the back region of the combustor. In the case of NO concentration, the value increases along the combustor axial direction and at the end of the combustor, 63.66ppm of NO is emitted.

5. Conclusions

Turbulent combustion flow and emissions distribution in the combustor were investigated with turbulent species library and Large Eddy Simulation (LES) numerical technique using personal servers clustered of 36 nodes with 12 CPU cores a node.

As the result of multiple injectors, premixed fuel flow in each in-jector with opposite swirl direction between adjacent injectors induces interaction among injectors. The corner and inter-space recirculation of neighbour injectors in multiple injector case is extremely complicated and unstable so that the flames from each injector concentrate inhomogeneous.

An analysis of the pollutant emission analysis, CO appears in the amount of 796.53ppm along the flame structure then disappears immediately after the flame. The CO formation on flame is relatively irregular compared to CO formation of single injectors. NO concentration is free from the flame structures and distributes homogeneously at the down-stream of the combustor. Due to remaining oxygen and nitrogen continuously react and generate NO so that NO concentration increases along the combustor axial direction.

References

- [1] A.C. Benim, K.J. Syed, 1998, "Laminar flamelet modelling of turbulent premixed combustion", *Mathematical Modelling*, Vol. 22, pp. 113~136.
- [2] Jung-Kyu Park, Truc Huu Nguyen, Min-Chul Lee, Jae-Wha Chung, 2012, "Prediction of pollutant emissions from premixed gas turbine combustor using chemical reactor network", *The Korean Society of Mechanical Engineers*, Vol. 36, No. 2, pp. 225~232.
- [3] Colin, O., Ducros, F., Veynante, D. and Poinot, T., 2002, "A Thickened Flame Model for Large Eddy Simulation of Turbulent Premixed Combustion," *Physics of Fluids*, Vol.12, pp. 1843-1863.

- [4] Kobayashi, H., Seyama, K., Hagiwara, H. and Ogami, Y., 2005, "Burning velocity correlation of methane/air turbulent premixed flames at high pressure and high temperature," *Proceedings of the Combustion Institute*, Vol. 30, pp. 827-834.
- [5] Huang, Y., and Yang, V., 2009, "Dynamics and stability of lean-premixed swirl-stabilized combustion," *Progress in Energy and Combustion Science*, Vol. 35, 2009, pp. 293-364.
- [6] Sung, H. G., 2007, "Combustion dynamics in a model lean-premixed gas turbine with a swirl stabilized injector," *Journal of Mechanical Science and Technology*, Vol. 21, No. 3, pp. 495-504.
- [7] Yoo, K. H., Kim, J. C., Sung, H.G., 2013, "Effects of cooling flow on the flow structure and acoustic oscillation in a swirl-stabilized combustor Part I. Flow characteristics," *Journal of Visualization*, Vol. 16, 287~295.